

# Recursive Dynamic State Estimation for Power Systems with an Incomplete Nonlinear DAE Model

Milos Katanic, John Lygeros, *Fellow, IEEE*, Gabriela Hug, *Senior Member, IEEE*

**Abstract**—Power systems are highly-complex, large-scale engineering systems subject to many uncertainties, which makes accurate mathematical modeling challenging. This paper proposes a novel, centralized dynamic state estimator for power systems that lack models of some components. Including the available dynamic evolution equations, algebraic network equations, and phasor measurements, we apply the least squares criterion to estimate all dynamic and algebraic states recursively. This approach results in an algorithm that generalizes the iterated extended Kalman filter and does not require static network observability. We further derive a graph theoretic condition to guarantee estimability for the proposed approach. A numerical study evaluates the performance under short circuits in the network and load changes for three different discretization schemes. The results show superior tracking performance compared to robust two-stage procedures within computational times that are feasible for real-time application.

**Index Terms**—Kalman filtering, under-determined power system differential algebraic model, PMU placement

## I. INTRODUCTION

STATIC state estimation (SSE) is an important component of energy management systems in power system control centers [1]. Traditionally, SSE relies on real-time measurement data obtained by the Supervisory Control and Data Acquisition (SCADA) system to calculate the most probable system state. Thereby, the system dynamics are disregarded due to slow scan rates and the asynchronous nature of the SCADA measurements.

Recent years have witnessed an increase in the deployment of phasor measurement units (PMUs), devices that directly measure current and voltage phasors at high sampling rates and time-stamp those measurements against a time reference obtained by the Global Positioning System. The advent of PMUs promoted the research interest in dynamic state estimation (DSE) for power systems. Even though the number of PMUs is constantly increasing, the growth rate in the North American power grid may have slowed down in the last few years, according to [2]. This fact motivates the development of state estimation methods that do not rely on static network observability by PMUs.

DSE for power systems has a rich and growing literature. Initial works considered only the swing dynamics of generators and completely neglected voltage dynamics in the

system [3]. Subsequently, the research community focused on the integration of dynamic models of generators and their controllers, thus still neglecting the estimation of the algebraic states (complex nodal voltages) [4]. Along this line, the most represented methods are the nonlinear variants of the Kalman filter: the extended Kalman filter [5], the unscented Kalman filter [6], and the particle filter [7]. Because of the inherent complexity of dealing with large-scale, nonlinear differential-algebraic equations (DAEs), researchers have leveraged index-1 characteristics of power system models to first propagate the differential states and subsequently solve the algebraic equations to obtain the voltage estimates [8]. However, this approach can only be applied if the model of the power system is fully known. Another simplification commonly employed is the Kron reduction [9], [10], which models the loads as prespecified impedances. An alternative approach that assumes static network observability is to use two-stage estimators where, in the first stage, only algebraic states are calculated, and subsequently, generators' dynamic states are estimated [11].

The implementation of DSE directly on the nonlinear DAE models is relatively recent. Along this line, [12] proposes a continuous time observer to simultaneously track differential and algebraic states. An extension to this observer to include also renewables generation is provided in [13]. Reference [14] shows that inequality constraints can be explicitly incorporated into the least squares estimation by reformulating them into equality constraints using complementarity theory. Finally, in our previous work [15], we address the problem in a moving-horizon fashion and deal with equality constraints and an incomplete power system model, albeit with a substantial computational burden.

One of the main challenges of the centralized DSE is the availability and complexity of accurate mathematical models [16]. Namely, power systems are large, heterogeneous, geographically wide-spread systems built incrementally over many decades. Consequently, they are often modeled by nonlinear equations of large dimensions spanning multiple time scales. Therefore, obtaining accurate models of all components is a daunting task. In addition, different areas of a power system are often operated by independent utilities, which may be reluctant to share models and measurement data. This problem may be exacerbated by the penetration of renewable energy sources as they are usually connected to the grid via vendor-specific power electronic converters, whose behavior is, to a large extent, dependent on the employed control algorithms. These companies may be unwilling to share details about their proprietary control software. Above all, various unan-

Research supported by the Swiss National Science Foundation under NCCR Automation, grant agreement 51NF40\_180545

Milos Katanic, John Lygeros, and Gabriela Hug are with the Information Technology and Electrical Engineering (D-ITET), ETH Zurich, 8092 Zurich, Switzerland (e-mail: mkatanic@ethz.ch; jlygeros@ethz.ch; hug@eeh.ee.ethz.ch).

anticipated disturbances and faults can occur, such as short circuits and line or load disconnections. It is unrealistic to assume that the operators can have real-time knowledge of all changes/disturbances occurring in the system.

The aforementioned difficulty has been recognized and addressed using decentralized state estimation or simplified models with robust estimators to subdue the effect of innovation or observation outliers. Decentralized state estimation aims to estimate the states of each generator separately [17]. The limitation of this method is that it requires the placement of a PMU on each generator terminal. In addition, the voltages at nodes where no generator is connected cannot be estimated. The second approach leverages short-term injection forecasts, historical records, or similar approximation methods to model loads or renewables infeed together with robust estimation schemes [18], [12]. This approach is similar to adding pseudo measurements with high covariance noise to SSE to restore observability when the network is unobservable. To deal with model and measurement uncertainties and unknown generator inputs, various robust estimators have been proposed [19]–[23]. However, robust estimation methods are usually computationally more expensive and more susceptible to numerical instabilities than ordinary least squares, which may prove prohibitive for real-time application. References [24] and [25] address the problem of an incomplete power system model, but both works are based on artificial neural networks; hence their out-of-sample performance is still to be validated. To the best of our knowledge, there exists, at present, no method for optimal recursive DSE for power systems with an under-determined nonlinear DAE model.

Our contributions can be summarized as follows:

- We devise a recursive, centralized least squares estimator for algebraic and dynamic state estimation for power systems with a partially known model. The estimator calculates the nodal voltages together with the internal states of all employed dynamic models. To derive the recursion, we extend the Kalman filtering for under-determined linear DAE systems from [26] to nonlinear cases resulting in a generalization of the iterated extended Kalman filter (IEKF). The estimation does not require the placement of PMUs at any specific bus type or the network to be statically observable. Moreover, it provides the possibility to gradually add new or remove existing models. Thus, for example, once a dynamic model of a generator or a load becomes available, it can be integrated into the estimation framework without redesigning the estimator. And vice versa, if a model proves suspicious, it can be removed, as long as estimability is still guaranteed.
- We address the problem of PMU placement and suggest a graph-theoretical criterion to guarantee topological estimability independent of the linearization point or system parameters. Estimability provides a guarantee that all system states can be uniquely estimated, given the available models and measurements (see [27] for a rigorous definition). We show that estimability can be achieved with fewer measurements than static network observability.
- The research community has for a long time largely

ignored the impact of the choice of the discretization scheme on the performance of DSE. Recently, [28] and [29] compared the accuracy of several different schemes. However, both works neglect the voltage excitation dynamics, which significantly contribute to the *stiffness* of the power systems model [30]. We compare the performance of the proposed estimation method for the explicit Euler, the implicit Euler, and the trapezoidal rule and conclude that the stiffness of the power system model can make the forward Euler method unsuitable for typical PMU sampling rates. We also validate the performance against a two-stage robust DSE and demonstrate superior tracking performance under transient conditions.

We define unknown injectors as all devices whose models are unknown and which inject positive or negative power into the network. The proposed method requires knowledge of the network topology and parameters in the area of interest for DSE. The rest of the system can be ignored and treated as an unknown injector. There exists in the literature a plethora of algorithms to estimate the network topology and parameters, using both conventional and phasor measurements (see [31] and the references therein). We also limit our analysis to fully balanced operating conditions.

The remainder of the paper is structured as follows. Section II proposes the estimation algorithm. Section III addresses the topological estimability condition. In Section IV, simulation results are discussed. Finally, Section V concludes the paper.

## II. ESTIMATION

### A. Kalman Filtering for Linear Discrete-Time Descriptor Systems

For improved readability, this subsection summarizes the most related results from [26], where a recursive optimal filter for a general class of linear discrete-time, stochastic descriptor systems of the form

$$\bar{E}\bar{x}_k = \bar{A}\bar{x}_{k-1} + \bar{\xi}_k, \quad (1)$$

$$\bar{z}_k = \bar{C}\bar{x}_k + \bar{\nu}_k, \quad (2)$$

is presented. Matrices  $\bar{E}$  and  $\bar{A}$  need not be invertible or even square: the method can handle under/over-constrained systems. It is assumed that  $\bar{\xi}_k$  and  $\bar{\nu}_k$  are zero mean white Gaussian noise sequences with

$$\mathbb{E} \left[ \begin{bmatrix} \bar{\xi}_k \\ \bar{\nu}_k \end{bmatrix} \begin{bmatrix} \bar{\xi}_j \\ \bar{\nu}_j \end{bmatrix}^T \right] = \begin{bmatrix} \bar{Q} & \mathbf{0} \\ \mathbf{0} & \bar{R} \end{bmatrix} \delta(k-j), \quad (3)$$

where  $\delta(l) = 1$  if  $l = 0$  and 0 otherwise.  $\bar{Q}$  and  $\bar{R}$  are positive definite covariance matrices. For the more general case with positive semi-definite covariance matrices, the interested reader is referred to [27]. The key idea is to process both the time-evolution equation (1) and the measurement equation (2) simultaneously in a batch-mode regression.

Denoting  $\hat{\bar{x}}_{k|j}$ ,  $k \leq j$ , as the estimate of  $\bar{x}_k$  once  $\bar{z}_j$  has been processed, and assuming  $\hat{\bar{x}}_{k-1|k-1}$ , and its covariance  $\bar{P}_{k-1|k-1} \succ \mathbf{0}$  are available, the optimal recursive state estimation at time step  $k$  can be formulated as the following optimization problem:

$$\min (\bar{\mathcal{A}}\bar{x} - \bar{\mathcal{B}})^T \bar{\mathcal{R}} (\bar{\mathcal{A}}\bar{x} - \bar{\mathcal{B}}), \quad (4)$$

where

$$\bar{\mathfrak{A}} := \begin{bmatrix} \bar{E} & \bar{A} \\ \bar{C} & \mathbf{0} \\ \mathbf{0} & \mathbf{I} \end{bmatrix}, \bar{\mathfrak{B}} := \begin{bmatrix} \mathbf{0} \\ \bar{z}_k \\ -\hat{\bar{x}}_{k-1|k-1} \end{bmatrix},$$

$$\bar{\mathfrak{K}} := \begin{bmatrix} \bar{Q}^{-1} & \mathbf{0} \\ \mathbf{0} & \bar{R}^{-1} \\ \mathbf{0} & \mathbf{0} \end{bmatrix}, \bar{\mathfrak{X}} := \begin{bmatrix} \bar{x}_k \\ -\bar{x}_{k-1} \end{bmatrix}.$$

If the matrix  $\begin{bmatrix} \bar{E} \\ \bar{C} \end{bmatrix}$  has full column rank, the optimal solution is given by [27]:

$$\hat{X} = (\bar{\mathfrak{A}}^T \bar{\mathfrak{K}} \bar{\mathfrak{A}})^{-1} \bar{\mathfrak{A}}^T \bar{\mathfrak{K}} \bar{\mathfrak{B}}, \quad (5)$$

or

$$\begin{bmatrix} \hat{\bar{x}}_{k|k} \\ \hat{\bar{x}}_{k-1|k} \end{bmatrix} = \begin{bmatrix} \bar{P}_{k|k} & \bar{P}_{k,k-1|k} \\ \bar{P}_{k,k-1|k}^T & \bar{P}_{k-1|k} \end{bmatrix} \begin{bmatrix} \bar{C}^T \bar{R}^{-1} \bar{z}_k \\ -\bar{P}_{k-1|k-1}^{-1} \hat{\bar{x}}_{k-1|k-1} \end{bmatrix}, \quad (6)$$

where

$$\begin{bmatrix} \bar{P}_{k|k} & \bar{P}_{k,k-1|k} \\ \bar{P}_{k,k-1|k}^T & \bar{P}_{k-1|k} \end{bmatrix} := \begin{bmatrix} \bar{E}^T \bar{Q}^{-1} \bar{E} + \bar{C}^T \bar{R}^{-1} \bar{C} & \bar{E}^T \bar{Q}^{-1} \bar{A} \\ \bar{A}^T \bar{Q}^{-1} \bar{E} & \bar{A}^T \bar{Q}^{-1} \bar{A} + \bar{P}_{k-1|k-1}^{-1} \end{bmatrix}^{-1}. \quad (7)$$

Notice that only  $\bar{P}_{k|k}$  and  $\bar{P}_{k,k-1|k}$  are needed to calculate the most recent state estimate. Applying the matrix inversion lemma and some algebraic transformations to (7) gives

$$\bar{P}_{k|k}^{-1} = \bar{E}^T (\bar{Q} + \bar{A} \bar{P}_{k-1|k-1} \bar{A}^T)^{-1} \bar{E} + \bar{C}^T \bar{R}^{-1} \bar{C},$$

$$\bar{P}_{k,k-1|k} = -\bar{P}_{k|k} \bar{E}^T (\bar{Q} + \bar{A} \bar{P}_{k-1|k-1} \bar{A}^T)^{-1} \bar{A} \bar{P}_{k-1|k-1}. \quad (8)$$

For details, the interested reader is referred to [32]. Substituting these expressions into (6) yields

$$\hat{\bar{x}}_{k|k} = \bar{P}_{k|k} \bar{E}^T (\bar{Q} + \bar{A} \bar{P}_{k-1|k-1} \bar{A}^T)^{-1} \bar{A} \hat{\bar{x}}_{k-1|k-1} + \bar{P}_{k|k} \bar{C}^T \bar{R}^{-1} \bar{z}_k. \quad (9)$$

For standard state space systems ( $\bar{E} = \mathbf{I}$ ), the recursion (8)–(9) reduces to the classical Kalman filter in the one-step form (see [33, p. 131]).

### B. Power System Dynamic State Estimation

Due to unknown components, the employed power system estimation model is under-determined. It is given by the following continuous-time, stochastic, under-constrained, nonlinear, semi-explicit DAE system:

$$\dot{\mathbf{y}} = \tilde{\mathbf{f}}(\mathbf{y}, \mathbf{v}) + \tilde{\boldsymbol{\xi}}_d, \quad (10)$$

$$\mathbf{0} = \tilde{\mathbf{g}}(\mathbf{y}, \mathbf{v}) + \tilde{\boldsymbol{\xi}}_a, \quad (11)$$

where  $\mathbf{y} \in \mathbb{R}^{n_d}$  and  $\mathbf{v} \in \mathbb{R}^{n_a}$  are respectively the vectors of the differential and algebraic states and  $\tilde{\mathbf{f}} : \mathbb{R}^{n_d+n_a} \rightarrow \mathbb{R}^{n_d}$  and  $\tilde{\mathbf{g}} : \mathbb{R}^{n_d+n_a} \rightarrow \mathbb{R}^{n_g}$ , with  $n_g < n_a$ , are nonlinear, differentiable, Lipschitz continuous functions representing the time evolution and algebraic nodal current balance equations in rectangular coordinates (see [30] for details).  $\tilde{\boldsymbol{\xi}}_d \in \mathbb{R}^{n_d}$  and  $\tilde{\boldsymbol{\xi}}_a \in \mathbb{R}^{n_g}$  are continuous-time Gaussian white noise vectors of independent random variables with  $\tilde{\boldsymbol{\xi}}_d \sim (\mathbf{0}, \tilde{\mathbf{Q}}_d)$  and

$\tilde{\boldsymbol{\xi}}_a \sim (\mathbf{0}, \tilde{\mathbf{Q}}_a)$ , where  $\tilde{\mathbf{Q}}_d \in \mathbb{R}^{n_d \times n_d}$  and  $\tilde{\mathbf{Q}}_a \in \mathbb{R}^{n_g \times n_g}$  are positive definite noise covariances. Internal states of individual dynamic models are coupled through the network, which is assumed to be connected. Inputs (set points) are not explicitly stated in (10)–(11), but are regarded as known parameters. As the number of states is larger than the number of equations, this system of equations is under-determined, and hence, the initial value problem (IVP) is not uniquely solvable. Therefore, we rely on time-discrete measurements to uniquely infer the system trajectory.

We use the following discrete-time representation:

$$\mathbf{y}_k = \mathbf{f}(\mathbf{y}_{k-1}, \mathbf{v}_{k-1}, \mathbf{y}_k, \mathbf{v}_k) h + \mathbf{y}_{k-1} + \boldsymbol{\xi}_{d,k}, \quad (12)$$

$$\mathbf{0} = \mathbf{g}(\mathbf{y}_k, \mathbf{v}_k) + \boldsymbol{\xi}_{a,k}, \quad (13)$$

$$\mathbf{z}_k = [\mathbf{0} \quad \mathbf{C}_2] \begin{bmatrix} \mathbf{y}_k \\ \mathbf{v}_k \end{bmatrix} + \boldsymbol{\nu}_k, \quad (14)$$

where  $\mathbf{f} : \mathbb{R}^{2n_d+2n_a} \rightarrow \mathbb{R}^{n_d}$  represents the discretized dynamics of (10),  $\mathbf{g}(\cdot) \equiv \tilde{\mathbf{g}}(\cdot)$ ,  $\mathbf{z}_k \in \mathbb{R}^{n_m}$  collects all PMU measurements,  $\mathbf{C} := [\mathbf{0} \quad \mathbf{C}_2] \in \mathbb{R}^{n_m \times (n_d+n_a)}$  is the output matrix of the linear PMU measurement function in rectangular coordinates [34],  $h \in \mathbb{R}^+$  denotes the discretization step size, and the subscript  $k \in \mathbb{Z}$  denotes the time instant. Discrete-time noise vectors  $\boldsymbol{\xi}_{d,k} \in \mathbb{R}^{n_d}$ ,  $\boldsymbol{\xi}_{a,k} \in \mathbb{R}^{n_g}$ , and  $\boldsymbol{\nu}_k \in \mathbb{R}^{n_m}$  are assumed to be independent Gaussian zero mean with

$$\mathbb{E} \begin{bmatrix} \begin{bmatrix} \boldsymbol{\xi}_{d,k} \\ \boldsymbol{\xi}_{a,k} \\ \boldsymbol{\nu}_k \end{bmatrix} \begin{bmatrix} \boldsymbol{\xi}_{d,j} \\ \boldsymbol{\xi}_{a,j} \\ \boldsymbol{\nu}_j \end{bmatrix}^T \end{bmatrix} = \begin{bmatrix} \mathbf{Q}_d & \mathbf{0} & \mathbf{0} \\ \mathbf{0} & \mathbf{Q}_a & \mathbf{0} \\ \mathbf{0} & \mathbf{0} & \mathbf{R} \end{bmatrix} \delta(k-j), \quad (15)$$

where  $\mathbf{Q}_d \in \mathbb{R}^{n_d \times n_d} \succ 0$ ,  $\mathbf{Q}_a \in \mathbb{R}^{n_g \times n_g} \succ 0$ ,  $\mathbf{R} \in \mathbb{R}^{n_m \times n_m} \succ 0$ . Note that the process noise  $\boldsymbol{\xi}_{d,k}$  may be non-zero mean as it also incorporates a discretization error which is difficult to quantify. This error, in general, also depends on the voltage evolution between the measurement samples; however, for deriving the optimal recursive filter, we ignore these attributes. In (14), conventional measurement devices, such as remote terminal units, are not considered as their slow scan rate and the lack of synchronization hinder their employment during transient conditions [16]. Formulation (12) subsumes several one-step discretization methods, such as the explicit Euler, the implicit Euler, and the trapezoidal rule.

We extend the approach outlined in Section II-A to nonlinear systems by first linearizing the dynamic equations and subsequently applying the optimal recursive filtering to the obtained affine system. Furthermore, we propose to apply the scheme several times iteratively, where each iteration yields a new (better) state estimate and hence a better linearization point. In the literature, such iterative estimation procedure is called the iterated extended Kalman filter (IEKF) [33]. The idea is that the successive linearization will render the linearization error negligible compared to noise. The approach is very similar to applying the Gauss-Newton method to solve the original nonlinear optimization problem [35].

We assume that the estimate  $(\hat{\mathbf{y}}_{k-1|k-1}, \hat{\mathbf{v}}_{k-1|k-1})$  and its covariance  $\mathbf{P}_{k-1|k-1} \in \mathbb{R}^{(n_d+n_a) \times (n_d+n_a)} \succ 0$  are available. First note that (12)–(13) need to be linearized around the previous estimate  $(\hat{\mathbf{y}}_{k-1|k-1}, \hat{\mathbf{v}}_{k-1|k-1})$ , but also around the current

iterate  $i$  of the current estimate  $(\hat{\mathbf{y}}_{k|k}^{(i)}, \hat{\mathbf{v}}_{k|k}^{(i)})$ . The initial iterate of the current time step can be obtained by setting it equal to the previous estimate, i.e.,  $\hat{\mathbf{y}}_{k|k}^{(0)} = \hat{\mathbf{y}}_{k-1|k-1}$ ,  $\hat{\mathbf{v}}_{k|k}^{(0)} = \hat{\mathbf{v}}_{k-1|k-1}$ . The Taylor series linearization of (12)–(13) around  $(\hat{\mathbf{y}}_{k-1|k-1}, \hat{\mathbf{v}}_{k-1|k-1}, \hat{\mathbf{y}}_{k|k}^{(i)}, \hat{\mathbf{v}}_{k|k}^{(i)})$  gives:

$$\begin{aligned} \mathbf{y}_k &\approx h\mathbf{f}(\hat{\mathbf{y}}_{k-1|k-1}, \hat{\mathbf{v}}_{k-1|k-1}, \hat{\mathbf{y}}_{k|k}^{(i)}, \hat{\mathbf{v}}_{k|k}^{(i)}) \\ &+ h\frac{\partial \mathbf{f}}{\partial \mathbf{y}_{k-1}}(\mathbf{y}_{k-1} - \hat{\mathbf{y}}_{k-1|k-1}) \\ &+ h\frac{\partial \mathbf{f}}{\partial \mathbf{v}_{k-1}}(\mathbf{v}_{k-1} - \hat{\mathbf{v}}_{k-1|k-1}) \\ &+ h\frac{\partial \mathbf{f}}{\partial \mathbf{y}_k}(\mathbf{y}_k - \hat{\mathbf{y}}_{k|k}^{(i)}) + h\frac{\partial \mathbf{f}}{\partial \mathbf{v}_k}(\mathbf{v}_k - \hat{\mathbf{v}}_{k|k}^{(i)}) \\ &+ \mathbf{y}_{k-1} + \boldsymbol{\xi}_{d,k}, \end{aligned} \quad (16)$$

$$\begin{aligned} \mathbf{0} &\approx \mathbf{g}(\hat{\mathbf{y}}_{k|k}^{(i)}, \hat{\mathbf{v}}_{k|k}^{(i)}) + \frac{\partial \mathbf{g}}{\partial \mathbf{y}_k}(\mathbf{y}_k - \hat{\mathbf{y}}_{k|k}^{(i)}) \\ &+ \frac{\partial \mathbf{g}}{\partial \mathbf{v}_k}(\mathbf{v}_k - \hat{\mathbf{v}}_{k|k}^{(i)}) + \boldsymbol{\xi}_{a,k}. \end{aligned} \quad (17)$$

In what follows, we omit the iteration superscript  $i$  as the analysis focuses on one single iteration of the algorithm. Introducing auxiliary variables for the Jacobians

$$\begin{aligned} \mathbf{A}_{1,k-1} &:= \frac{\partial \mathbf{f}}{\partial \mathbf{y}_{k-1}} \in \mathbb{R}^{n_d \times n_d}, & \mathbf{A}_{2,k-1} &:= \frac{\partial \mathbf{f}}{\partial \mathbf{v}_{k-1}} \in \mathbb{R}^{n_d \times n_a}, \\ \mathbf{E}_{1,k} &:= \frac{\partial \mathbf{f}}{\partial \mathbf{y}_k} \in \mathbb{R}^{n_d \times n_d}, & \mathbf{E}_{2,k} &:= \frac{\partial \mathbf{f}}{\partial \mathbf{v}_k} \in \mathbb{R}^{n_d \times n_a}, \\ \mathbf{E}_{3,k} &:= \frac{\partial \mathbf{g}}{\partial \mathbf{y}_k} \in \mathbb{R}^{n_g \times n_d}, & \mathbf{E}_{4,k} &:= \frac{\partial \mathbf{g}}{\partial \mathbf{v}_k} \in \mathbb{R}^{n_g \times n_a}, \end{aligned}$$

and concatenating

$$\begin{aligned} \mathbf{x}_k &:= \begin{bmatrix} \mathbf{y}_k \\ \mathbf{v}_k \end{bmatrix} \in \mathbb{R}^{n_d+n_a}, \quad \boldsymbol{\xi}_k := \begin{bmatrix} \boldsymbol{\xi}_{d,k} \\ \boldsymbol{\xi}_{a,k} \end{bmatrix} \in \mathbb{R}^{n_d+n_g}, \\ \mathbf{Q} &:= \begin{bmatrix} \mathbf{Q}_d & \mathbf{0} \\ \mathbf{0} & \mathbf{Q}_a \end{bmatrix} \in \mathbb{R}^{(n_d+n_g) \times (n_d+n_g)}, \end{aligned} \quad (18)$$

allows us to rewrite (16)–(17) and (14) as

$$\mathbf{E}_k \mathbf{x}_k \approx \mathbf{A}_{k-1} \mathbf{x}_{k-1} + \boldsymbol{\Delta}_k + \boldsymbol{\xi}_k, \quad (19)$$

$$\mathbf{z}_k = \mathbf{C} \mathbf{x}_k + \boldsymbol{\nu}_k, \quad (20)$$

where  $\mathbf{E}_k$ ,  $\mathbf{A}_{k-1}$ , and  $\boldsymbol{\Delta}_k$  are defined in (21).

We can now formulate the optimization problem to calculate the state estimate at time step  $k$  as

$$\min (\mathfrak{A}\boldsymbol{\mathcal{X}} - \mathfrak{B})^T \mathfrak{R} (\mathfrak{A}\boldsymbol{\mathcal{X}} - \mathfrak{B}), \quad (22)$$

where

$$\begin{aligned} \mathfrak{A} &:= \begin{bmatrix} \mathbf{E}_k & \mathbf{A}_{k-1} \\ \mathbf{C} & \mathbf{0} \\ \mathbf{0} & \mathbf{I} \end{bmatrix}, \quad \mathfrak{B} := \begin{bmatrix} \boldsymbol{\Delta}_k \\ \mathbf{z}_k \\ -\hat{\mathbf{x}}_{k-1|k-1} \end{bmatrix}, \\ \mathfrak{R} &:= \begin{bmatrix} \mathbf{Q}^{-1} & \mathbf{0} & \mathbf{0} \\ \mathbf{0} & \mathbf{R}^{-1} & \mathbf{0} \\ \mathbf{0} & \mathbf{0} & \mathbf{P}_{k-1|k-1}^{-1} \end{bmatrix}, \quad \boldsymbol{\mathcal{X}} := \begin{bmatrix} \mathbf{x}_k \\ -\mathbf{x}_{k-1} \end{bmatrix}. \end{aligned} \quad (23)$$

Notice the additional term  $\boldsymbol{\Delta}_k$  introduced by the linearization. Under the assumption of the full column rank of  $\begin{bmatrix} \mathbf{E}_k \\ \mathbf{C} \end{bmatrix}$  the minimum is attained at

$$\hat{\boldsymbol{\mathcal{X}}} = (\mathfrak{A}^T \mathfrak{R} \mathfrak{A})^{-1} \mathfrak{A}^T \mathfrak{R} \mathfrak{B}, \quad (24)$$

or

$$\begin{aligned} \begin{bmatrix} \hat{\mathbf{x}}_{k|k} \\ \hat{\mathbf{x}}_{k-1|k} \end{bmatrix} &= \begin{bmatrix} \mathbf{P}_{k|k} & \mathbf{P}_{k,k-1|k} \\ \mathbf{P}_{k,k-1|k}^T & \mathbf{P}_{k-1|k} \end{bmatrix} \\ &\begin{bmatrix} \mathbf{C}^T \mathbf{R}^{-1} \mathbf{z}_k + \mathbf{E}_k^T \mathbf{Q}^{-1} \boldsymbol{\Delta}_k \\ -\mathbf{P}_{k-1|k-1}^{-1} \hat{\mathbf{x}}_{k-1|k-1} + \mathbf{A}_{k-1}^T \mathbf{Q}^{-1} \boldsymbol{\Delta}_k \end{bmatrix}. \end{aligned} \quad (25)$$

To simplify the notation, we drop the subscript after the vertical bar, as it is implicitly clear from the time step at which an estimate was obtained. As we are only interested in the estimation of the most recent state of the system  $\hat{\mathbf{x}}_k$ , rewriting the terms from the linear case (9) and including the additional terms introduced by the linearization gives

$$\begin{aligned} \hat{\mathbf{x}}_k &\stackrel{(1)}{=} \mathbf{P}_k \mathbf{E}^T (\mathbf{Q} + \mathbf{A} \mathbf{P}_{k-1} \mathbf{A}^T)^{-1} \mathbf{A} \hat{\mathbf{x}}_{k-1} \\ &\quad + \mathbf{P}_k \mathbf{H}^T \mathbf{R}^{-1} \mathbf{z}_k + \mathbf{P}_k \mathbf{E}^T \mathbf{Q}^{-1} \boldsymbol{\Delta}_k \\ &\quad - \mathbf{P}_k \mathbf{E}^T (\mathbf{Q} + \mathbf{A} \mathbf{P}_{k-1} \mathbf{A}^T)^{-1} \mathbf{A} \mathbf{P}_{k-1} \mathbf{A}^T \mathbf{Q}^{-1} \boldsymbol{\Delta}_k \\ &\stackrel{(2)}{=} \mathbf{P}_k \mathbf{E}^T (\mathbf{Q} + \mathbf{A} \mathbf{P}_{k-1} \mathbf{A}^T)^{-1} \mathbf{A} \hat{\mathbf{x}}_{k-1} \\ &\quad + \mathbf{P}_k \mathbf{H}^T \mathbf{R}^{-1} \mathbf{z}_k + \mathbf{P}_k \mathbf{E}^T \cdot \\ &\quad \{ \mathbf{Q}^{-1} - (\mathbf{Q} + \mathbf{A} \mathbf{P}_{k-1} \mathbf{A}^T)^{-1} \mathbf{A} \mathbf{P}_{k-1} \mathbf{A}^T \mathbf{Q}^{-1} \} \boldsymbol{\Delta}_k \\ &\stackrel{(3)}{=} \mathbf{P}_k \mathbf{E}^T (\mathbf{Q} + \mathbf{A} \mathbf{P}_{k-1} \mathbf{A}^T)^{-1} \mathbf{A} \hat{\mathbf{x}}_{k-1} \\ &\quad + \mathbf{P}_k \mathbf{H}^T \mathbf{R}^{-1} \mathbf{z}_k + \mathbf{P}_{k|k} \mathbf{E}^T \{ (\mathbf{Q} + \mathbf{A} \mathbf{P}_{k-1} \mathbf{A}^T)^{-1} \cdot \\ &\quad [ (\mathbf{Q} + \mathbf{A} \mathbf{P}_{k-1} \mathbf{A}^T) \mathbf{Q}^{-1} - \mathbf{A} \mathbf{P}_{k-1} \mathbf{A}^T \mathbf{Q}^{-1} ] \} \boldsymbol{\Delta}_k \\ &\stackrel{(4)}{=} \mathbf{P}_k \mathbf{E}^T (\mathbf{Q} + \mathbf{A} \mathbf{P}_{k-1} \mathbf{A}^T)^{-1} \mathbf{A} \hat{\mathbf{x}}_{k-1} \\ &\quad + \mathbf{P}_k \mathbf{H}^T \mathbf{R}^{-1} \mathbf{z}_k + \mathbf{P}_k \mathbf{E}^T (\mathbf{Q} + \mathbf{A} \mathbf{P}_{k-1} \mathbf{A}^T)^{-1} \boldsymbol{\Delta}_k. \end{aligned} \quad (26)$$

The second equality follows from factoring out  $\mathbf{P}_k \mathbf{E}^T$  and  $\boldsymbol{\Delta}_k$  in the third and fourth summand, the third equality follows by factoring out  $(\mathbf{Q} + \mathbf{A} \mathbf{P}_{k-1} \mathbf{A}^T)^{-1}$  in the curly brackets, and the fourth equality follows from the associativity of matrix

---


$$\begin{aligned} \mathbf{E}_k &:= \begin{bmatrix} h\mathbf{E}_{1,k} - \mathbf{I} & h\mathbf{E}_{2,k} \\ \mathbf{E}_{3,k} & \mathbf{E}_{4,k} \end{bmatrix} \in \mathbb{R}^{(n_d+n_g) \times (n_d+n_a)}, \quad \mathbf{A}_{k-1} := \begin{bmatrix} -h\mathbf{A}_{1,k-1} - \mathbf{I} & -h\mathbf{A}_{2,k-1} \\ \mathbf{0} & \mathbf{0} \end{bmatrix} \in \mathbb{R}^{(n_d+n_g) \times (n_d+n_a)}, \\ \boldsymbol{\Delta}_k &:= \begin{bmatrix} h\mathbf{E}_{1,k} \hat{\mathbf{x}}_{k|k} + h\mathbf{E}_{2,k} \hat{\mathbf{v}}_{k|k} + h\mathbf{A}_{1,k-1} \hat{\mathbf{x}}_{k-1|k-1} + h\mathbf{A}_{2,k-1} \hat{\mathbf{v}}_{k-1|k-1} - h\mathbf{f}(\hat{\mathbf{y}}_{k-1|k-1}, \hat{\mathbf{v}}_{k-1|k-1}, \hat{\mathbf{y}}_{k|k}^{(i)}, \hat{\mathbf{v}}_{k|k}^{(i)}) \\ \mathbf{E}_{3,k} \hat{\mathbf{x}}_{k|k} + \mathbf{E}_{4,k} \hat{\mathbf{v}}_{k|k} - \mathbf{g}(\hat{\mathbf{y}}_{k|k}^{(i)}, \hat{\mathbf{v}}_{k|k}^{(i)}) \end{bmatrix} \in \mathbb{R}^{n_d+n_g}. \end{aligned} \quad (21)$$

multiplication. Hence, the final expression is given by the following recursion:

$$\begin{aligned}\hat{\mathbf{x}}_k &= \mathbf{P}_k \mathbf{E}_k^T (\mathbf{Q} + \mathbf{A}_{k-1} \mathbf{P}_{k-1} \mathbf{A}_{k-1}^T)^{-1} \\ &\quad (\mathbf{A} \hat{\mathbf{x}}_{k-1} + \Delta_k) + \mathbf{P}_k \mathbf{C}^T \mathbf{R}^{-1} \mathbf{z}_k, \\ \mathbf{P}_k^{-1} &= \mathbf{E}_k^T (\mathbf{Q} + \mathbf{A}_{k-1} \mathbf{P}_{k-1} \mathbf{A}_{k-1}^T)^{-1} \mathbf{E}_k + \mathbf{C}^T \mathbf{R}^{-1} \mathbf{C}.\end{aligned}\quad (27)$$

If  $\mathbf{f}$  and  $\mathbf{g}$  are linear,  $\Delta_k = \mathbf{0}$ , and the recursion coincides with (9).

Finally, we execute the algorithm iteratively in the form of the IEKF. Applying (27) gives the new estimate iterate  $\hat{\mathbf{x}}_k^{(i)}$ . The Jacobians can be reevaluated for this estimate, and the procedure repeated until convergence; as a termination criterion we can take  $\left\| \hat{\mathbf{x}}_k^{(i)} - \hat{\mathbf{x}}_k^{(i-1)} \right\|_{\infty} \leq \epsilon$ , for a small  $\epsilon > 0$ . Algorithm 1 provides the pseudo-code of the proposed IEKF for time step  $k$ .

---

**Algorithm 1** IEKF for under-determined DAE systems

---

**Input:**  $\hat{\mathbf{x}}_{k-1|k-1}, \mathbf{P}_{k-1|k-1}$

**Output:**  $\hat{\mathbf{x}}_{k|k}, \mathbf{P}_{k|k}$

Calculate  $\mathbf{A}_{k-1}$  from (21)

$i \leftarrow 0$

$\hat{\mathbf{x}}_{k|k}^{(0)} \leftarrow \hat{\mathbf{x}}_{k-1|k-1}$

**do**

$i \leftarrow i + 1$

Calculate  $\mathbf{E}_k^{(i)}, \Delta_k^{(i)}$  from (21)

Apply recursion (27) to calculate  $\hat{\mathbf{x}}_{k|k}^{(i)}$  and  $\hat{\mathbf{P}}_{k|k}^{(i)}$

**while**  $\left\| \hat{\mathbf{x}}_{k|k}^{(i)} - \hat{\mathbf{x}}_{k|k}^{(i-1)} \right\|_{\infty} > \epsilon$

$\hat{\mathbf{x}}_{k|k} \leftarrow \hat{\mathbf{x}}_{k|k}^{(i)}$

$\hat{\mathbf{P}}_{k|k} \leftarrow \hat{\mathbf{P}}_{k|k}^{(i)}$

---

### III. ESTIMABILITY ANALYSIS

This section analyzes the estimability conditions for the proposed method. In what follows, we drop the subscript  $k$  from the matrices in (21) to simplify the notation. Estimability refers to the ability of uniquely determining all state estimates given the dynamics and the measurement equations, or in other words: it refers to the existence of the unique minimizer of (22). It follows from [27] that the sufficient and necessary condition for estimability is that the matrix  $\begin{bmatrix} \mathbf{E} \\ \mathbf{C} \end{bmatrix}$  is full column rank, a condition known as fast subsystem observability in the linear descriptor systems literature [36]. We now show that it is sufficient to certify the full rank of  $\begin{bmatrix} \mathbf{E}_4 \\ \mathbf{C}_2 \end{bmatrix}$  to satisfy the estimability condition.

**Lemma 1.** *For sufficiently small discretization steps  $h$ , full column rank of the matrix  $\begin{bmatrix} \mathbf{E}_4 \\ \mathbf{C}_2 \end{bmatrix}$  implies full column rank of the matrix  $\begin{bmatrix} \mathbf{E} \\ \mathbf{C} \end{bmatrix}$ .*

*Proof.* First, we introduce the following notation:

$$\tilde{\mathbf{E}}_3 := \begin{bmatrix} \mathbf{E}_3 \\ \mathbf{0} \end{bmatrix} \in \mathbb{R}^{(n_g+n_m) \times n_d}, \quad \tilde{\mathbf{E}}_4 := \begin{bmatrix} \mathbf{E}_4 \\ \mathbf{C}_2 \end{bmatrix} \in \mathbb{R}^{(n_g+n_m) \times n_a},$$

to rewrite  $\begin{bmatrix} \mathbf{E} \\ \mathbf{C} \end{bmatrix} = \begin{bmatrix} h\mathbf{E}_1 - \mathbf{I} & h\mathbf{E}_2 \\ \tilde{\mathbf{E}}_3 & \tilde{\mathbf{E}}_4 \end{bmatrix}$ . For sufficiently small  $h$ , the submatrix  $\begin{bmatrix} h\mathbf{E}_1 - \mathbf{I} \end{bmatrix}$  is full rank.

To complete the proof, assume for the sake of contradiction that the matrix  $\begin{bmatrix} \mathbf{E} \\ \mathbf{C} \end{bmatrix}$  is not full column rank. Then there exists a vector  $\begin{bmatrix} \mathbf{x}_1 \\ \mathbf{x}_2 \end{bmatrix} \neq \mathbf{0}$  of appropriate dimension such that

$$\begin{bmatrix} h\mathbf{E}_1 - \mathbf{I} & h\mathbf{E}_2 \\ \tilde{\mathbf{E}}_3 & \tilde{\mathbf{E}}_4 \end{bmatrix} \begin{bmatrix} \mathbf{x}_1 \\ \mathbf{x}_2 \end{bmatrix} = \begin{bmatrix} \mathbf{0} \\ \mathbf{0} \end{bmatrix}. \quad (28)$$

Expressing  $\mathbf{x}_1$  from the first equation of (28) as

$$\mathbf{x}_1 = h(\mathbf{I} - h\mathbf{E}_1)^{-1} \mathbf{E}_2 \mathbf{x}_2, \quad (29)$$

and substituting into the second gives

$$\left( h\tilde{\mathbf{E}}_3(\mathbf{I} - h\mathbf{E}_1)^{-1} \mathbf{E}_2 + \tilde{\mathbf{E}}_4 \right) \mathbf{x}_2 = \mathbf{0}. \quad (30)$$

Pre-multiplying (30) by  $\frac{1}{h} \left( \tilde{\mathbf{E}}_4^T \tilde{\mathbf{E}}_4 \right)^{-1} \tilde{\mathbf{E}}_4^T$  (the inverse exists because of full column rank of  $\tilde{\mathbf{E}}_4$ ) gives

$$\left( \left( \tilde{\mathbf{E}}_4^T \tilde{\mathbf{E}}_4 \right)^{-1} \tilde{\mathbf{E}}_4^T \tilde{\mathbf{E}}_3 (\mathbf{I} - h\mathbf{E}_1)^{-1} \mathbf{E}_2 + \frac{1}{h} \mathbf{I} \right) \mathbf{x}_2 = \mathbf{0}. \quad (31)$$

Because the Jacobians are bounded, and, for small  $h$ ,  $\begin{bmatrix} \mathbf{I} - h\mathbf{E}_1 \end{bmatrix}^{-1}$  is also bounded, as  $h \rightarrow 0$ , the eigenvalues of  $\frac{1}{h} \mathbf{I}$  are dominating, and the matrix from (31) is full rank. Consequently,  $\mathbf{x}_2 = \mathbf{0}$ , and from (29), it follows that  $\mathbf{x}_1 = \mathbf{0}$ , which is a contradiction and therefore concludes the proof.  $\square$

Lemma 1 suggests that the placement of PMUs should ensure full rank of  $\begin{bmatrix} \mathbf{E}_4 \\ \mathbf{C}_2 \end{bmatrix}$ . This requirement is addressed in the next subsection. Also note that if all component models are available,  $\mathbf{E}_4$  is a square matrix, and the full rank criterion follows from the DAE model being (locally) of differentiation index-1 [37]. Hence, if the power system is modeled such that no impulse terms can appear as a response to step changes in input signals or inconsistent initial conditions, the estimability condition is satisfied even without any measurements, or in other words, the IVP can be uniquely solved without relying on time-discrete observations.

#### A. Graphs of Structured Matrices

The estimability criterion ensures, statistically speaking, the availability of a sufficient amount of information to uniquely estimate all differential  $\mathbf{y}_k$  and algebraic states  $\mathbf{v}_k$  at all times. A direct computation of the rank of the given matrix is not only computationally expensive for large power systems but more importantly, it does not provide any intuition about why the given sensor placement does not guarantee estimability nor where additional sensors should be placed to restore it. Instead, inspired by [38] and [39], where a topological criterion for static observability and a dynamic observer based on graph theory are presented, we aim to develop an algorithm that can be applied to any network and does not depend on the specific network parameters but only on the topological structure of the underlying grid. To this end, we introduce the concept of structured matrices.

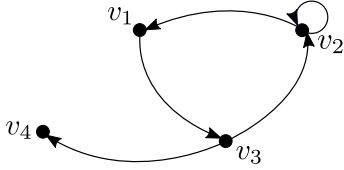


Fig. 1. Graph of the structured pair  $(\mathcal{E}, \mathcal{C})$

A structured matrix is a matrix whose elements are either fixed zeros or non-zero indeterminate (free) parameters. The generic rank of a structured matrix is defined as the maximal rank it can reach as a function of its free parameters. In [40], it was shown that the rank of a given matrix equals its generic rank except for pathological cases with Lebesgue measure zero. Such cases are unlikely to occur in practice, and even if they did, an arbitrary small perturbation of the parameters restores the maximal rank [40]. In SSE for power systems, such pathological cases are referred to as parametric unobservability [38]. However, if the measurement Jacobian is generically full rank, the system is still called topologically observable. Analogously, we refer to the full generic rank of  $\begin{bmatrix} \mathcal{E}_4 \\ \mathcal{C}_2 \end{bmatrix}$  as the *topological estimability* criterion for the proposed DSE.

We introduce a structured system as a pair of structured matrices  $(\mathcal{E}, \mathcal{C})$ , where  $\mathcal{E} \in \mathbb{R}^{n \times n}$  and  $\mathcal{C} \in \mathbb{R}^{m \times n}$ . To each structured system, a directed graph can be associated in the following way: the graph of the given pair  $(\mathcal{E}, \mathcal{C})$  contains  $n + m$  vertices, denoted  $v_1, v_2, \dots, v_{n+m}$ . For each free parameter  $a_{ij}$  where  $i \in 1, \dots, n+m$  and  $j \in 1, \dots, n$  of the structured system, there exists an oriented edge from  $v_j$  to  $v_i$  in the graph representation. To facilitate the understanding, let us introduce an example of a structured pair.

*Example:* Let

$$\mathcal{E} = \begin{bmatrix} 0 & a_{12} & 0 \\ 0 & a_{22} & a_{23} \\ a_{31} & 0 & 0 \end{bmatrix}, \quad \mathcal{C} = \begin{bmatrix} 0 & 0 & a_{43} \end{bmatrix}. \quad (32)$$

The associated graph is given in Fig. 1. Notice that the vertices corresponding to the rows of  $\mathcal{C}$  are all sink vertices as no edge points outwards from them; we call all paths ending in such vertices  $\mathcal{C}$ -topped paths.

We now state a theorem from [40] useful for analyzing topological estimability of power systems.

**Theorem 2.** [40, Theorem 1] *Given structured matrices  $\mathcal{E} \in \mathbb{R}^{n \times n}$  and  $\mathcal{C} \in \mathbb{R}^{m \times n}$ , the matrix  $\begin{bmatrix} \mathcal{E} \\ \mathcal{C} \end{bmatrix}$  is generically full column rank if and only if there exists a disjoint union of loops and  $\mathcal{C}$ -topped paths that span all vertices of  $\mathcal{E}$  in the graph of the structured pair.*

Applying the previous theorem to the example in Fig. 1, we ascertain that  $\begin{bmatrix} \mathcal{E} \\ \mathcal{C} \end{bmatrix}$  is generically full column rank because its graph can be spanned by the simple path  $v_2 \rightarrow v_1 \rightarrow v_3 \rightarrow v_4$ . However, removing, for example, edge  $a_{31}$  renders the first column of  $\begin{bmatrix} \mathcal{E} \\ \mathcal{C} \end{bmatrix}$  a zero column and the graph  $\mathcal{E}$  cannot be spanned anymore by disjoint loops and  $\mathcal{C}$ -topped paths.

## B. Power Systems Topological Estimability

We now regard the pair  $(\mathbf{E}_4, \mathbf{C}_2)$  as structured matrices, by considering their non-zero entries (which depend on the power system parameters and operating point) as free parameters. Recall that the matrix  $\mathbf{E}_4$  is not square due to unknown models of some injectors. Therefore, we expand it by an appropriate number of zero rows, specifically two additional zero rows for each unknown injector (one for the real and one for the imaginary part). This augmentation does not alter the (generic) rank of the matrix.

As in the previous subsection, we can associate a graph with the pair  $(\mathbf{E}_4, \mathbf{C}_2)$ , with  $2(n_a + n_m)$  vertices and a structure similar to the power system topology. Henceforth, to make the distinction clearer, when we refer to the graph of the structured pair  $(\mathbf{E}_4, \mathbf{C}_2)$ , we use the terminology of vertices and edges, whereas for the topology of the corresponding power system, we use nodes and branches. Each node of the power system is represented by two vertices in the graph representation; we call them the real and the imaginary vertex of the corresponding power system node. By definition,  $\mathbf{E}_4$  is the Jacobian of the algebraic current balance equations with respect to the complex voltages expressed in rectangular coordinates. Therefore,  $\mathbf{E}_4$  has a similar structure to the power system admittance matrix, but the rows corresponding to the nodes with unknown injectors are replaced by zero rows, and the sensitivities of the dynamic models are added. Hence, there exists a free parameter in  $\mathbf{E}_4$  if and only if the real/imaginary current balance equation in a particular node depends on the real/imaginary voltage of another node. It follows that there exist edges in the graph of the structured system only between neighboring nodes of the power system. Furthermore, all edges in the corresponding graph are bidirectional, except for the edges originating from the vertices corresponding to the nodes with unknown injectors (the corresponding rows in matrix  $\mathbf{E}_4$  are zero rows), and the edges leading to measurement vertices. Moreover, if two nodes  $i$  and  $j$  are connected by a transmission line with conductance  $G_{ij} \neq 0$ , there exist edges between the real vertices of the corresponding nodes; if the susceptance  $B_{ij} \neq 0$ , there exist edges between the real and the imaginary vertices of the corresponding nodes. Shunt elements correspond to either a loop around a vertex itself or an edge from its real/imaginary counterpart and also they ensure the independence of the entries in each row of  $\mathbf{E}_4$ .

To state the main theorem of the subsection, we need to define a representation of the phasor measurements in the power system topology. We assign each voltage phasor measurement to the node at which it is placed; the branch current flow measurements are assigned to either of the two nodes defining the branch, and the current injection measurements are assigned to the respective node or to any of its neighboring nodes. This selection is a consequence of the respective measurement functions  $\mathbf{C}_2$  [34] and the fact that there can only be one path ending at each  $\mathbf{C}_2$  vertex to satisfy the conditions of Theorem 2.

**Theorem 3.** *The power system (12)–(14) is topologically estimable by (27) if there exist disjoint paths along transmission lines from all nodes with an unknown injector to a node with*

an assigned PMU device.

*Proof.* By Theorem 2, we only need to show that, under the given assumptions,  $\mathbf{E}_4$  vertices in the graph representation of  $(\mathbf{E}_4, \mathbf{C}_2)$  can be spanned by a disjoint union of loops and  $\mathbf{C}_2$ -topped paths. Indeed, starting from the origin vertices (corresponding to the nodes with unknown injectors), we move in the same way as in the power systems topology with the slight modification that we need to traverse twice as many edges as transmission lines. Thus, whenever we move along a transmission line from node  $i$  to node  $j$  with  $G_{ij} \neq 0$ , we move from the real vertex of node  $i$  to the real vertex of  $j$  and from the imaginary vertex of  $i$  to the imaginary vertex of  $j$ ; if  $B_{ij} \neq 0$ , we move from the real to the imaginary and from the imaginary to the real vertex; if  $G_{ij}B_{ij} \neq 0$ , we can choose either of the two options. Once a node with an assigned measurement device is reached, we also reached a  $\mathbf{C}_2$  sink vertex for both paths, as we assume that all PMUs measure both real and imaginary components. In this way, all the paths stay disjoint. Recall that there are only outward-going edges from a vertex with an unknown injector and only inward-going edges towards a measurement vertex, and they are both traversed in the correct direction. Now we only need to span the remaining vertices that have not been traversed so far. Those remaining vertices correspond to the nodes with the known injectors' dynamic models or zero injection nodes, hence to nonzero rows in matrix  $\mathbf{E}_4$ . As such, they can either be spanned by trivial loops around themselves or around their real/imaginary counterpart vertex.  $\square$

We note that the previous analysis is valid irrespective of the employed dynamic models. To show that, observe that the sensitivities of the dynamic models' current injections are only a function of the voltage of that node. Hence, these values are added to a corresponding  $2 \times 2$  submatrix, where the diagonal or off-diagonal entries – due to at least one incoming transmission line – enable forming a loop around both vertices.

The above analysis provides a method to verify estimability of the DSE, however, it does not suggest how to optimally place PMUs to achieve a specific performance metric. This can be potentially achieved by formulating a combinatorial optimization problem that may be amenable to submodular optimization techniques – a topic for future work.

## IV. NUMERICAL RESULTS

### A. Simulation Setup

To validate the performance of the proposed method, we perform numerical simulations on a power system comprising synchronous generators (SG), loads, and a network interconnecting them. The presented algorithm is not limited to such models, and the extension to a system with renewable generation is part of future work.

The IEEE 39-bus test system is used, whose parameters are taken from [41]. The goal is to perform the state estimation on the shaded area depicted in Fig. 2. From the perspective of the operator of this area, the rest of the power system is out of interest. Hence, interface node 16 can be considered as a node with an unknown dynamic model by the proposed estimation

scheme and only the topology and network parameters of the shaded area are needed for the DSE.

The ground-truth values are obtained by a simulation that employs the subtransient synchronous generator model [42] including the IEEE DC1A automatic voltage regulator [42] and the simple TGOV1 turbine model [43]. The subtransient reactances are set to 90% of their transient counterparts, whereas the subtransient time constants are 100 times smaller than the transient counterparts [44]. All loads are modeled as a composition of a negative power injection and an impedance.

For the estimation, we use the two-axis, transient model of the synchronous generator [45] to take into account that mathematical models only represent a simplified description of the true behavior of a physical system. We assume that the exciter and the turbine model and the generators' power and voltage set points are known. However, we consider all load models/consumption unknown to the estimator. Obtaining their accurate models is difficult in practice, and modeling them as static consumers with their power inferred from historical data may be unreliable, especially during disturbances and transient events [46]. In case dynamic models or reliable real-time consumption data are available, they can be incorporated into the framework in a straightforward manner. Therefore, for the proposed estimator, nodes 16, 20, 21, 23, and 24 are nodes with unknown injectors, which makes the estimation model incomplete. We assume no prior knowledge and make no assumptions regarding the injections of these nodes. PMU measurements are assumed to arrive simultaneously every 20 ms [47]; their values are obtained by adding Gaussian measurement noise with a standard deviation of 0.001 pu to the real and imaginary voltage and current ground-truth values. PMU voltage measurements are placed at nodes 19, 23, and 34; PMU branch current measurements are located at lines 16 – 19, 16 – 24, and 22 – 23. We assign the PMU at line 16 – 24 to node 24, and the PMU at line 22 – 23 to node 22 and observe that topological estimability for the proposed method is satisfied as all unknown injectors can be connected to a node with an assigned PMU device by disjoint paths: injector 16 to node 16, injector 20 to node 34, injector 21 to node 22, injector 23 to node 23, and finally injector 24 to node 24 (see Fig. 2). By contrast, the power system is statically not observable, or, more precisely, ignoring the dynamic equations, the voltages are not uniquely estimable from the given PMU measurements.

All simulations are implemented in Python on an Intel i7-10510U CPU @ 1.80GHz with 16GB RAM. Cholesky factorization is used to factorize the state estimation covariance matrix in (27), which can be ill-conditioned. All Jacobians are computed by the algorithmic differentiation using CasADi's symbolic framework [48].

### B. Case Study 1: Network Short Circuit

Short circuits are one of the most severe disturbances with respect to their impact on power system stability, but also with respect to the stability of the implemented numerical methods for simulation. Here, we simulate a three-phase short circuit at  $t = 8$  s in the middle between two PMU sampling events on

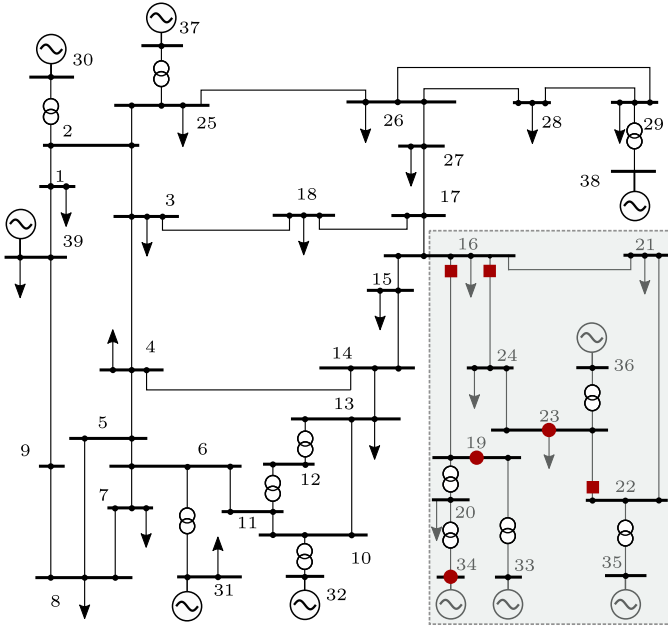


Fig. 2. Single line diagram of the IEEE 39-bus test system. The estimation is performed on the shaded area. Voltage phasor measurements are denoted by the red circles and current phasor measurements by the red squares.

TABLE I  
COMPUTATIONAL PERFORMANCE OF THE PROPOSED DSE FOR THREE  
DISCRETIZATION METHODS AT EACH PMU SCAN

	Forward Euler	Backward Euler	Trapezoidal
$t_{avg}$	2.1 ms	2.4 ms	2.4 ms
$t_{max}$	5.0 ms	6.2 ms	5.3 ms
Max. iterations	4	2	2

the line between nodes 5 and 8, which is cleared after 60 ms on both ends. Note that the operator of the shaded area from Fig. 2 (and hence the proposed estimator) has no direct awareness of this disturbance. The estimation is initialized with a voltage flat start; the differential states are initialized with a Gaussian random error from the ground-truth with a standard deviation of 1%, except for the rotor speeds, where the deviation is 0.05%.

The results for the rotor angle, rotor speed, turbine power, and exciter voltage for the generators at nodes 33, 34, and 36 are shown in Fig. 3. All rotor angles are given with respect to the rotor angle at bus 34. It can be seen that both the implicit Euler and the trapezoidal rule achieve excellent tracking performance once they have converged from their initialization to the pre-fault state of the system, whereas the explicit Euler suffers from oscillatory behavior, making it unsuitable for the tested scenario of a severe disturbance when the network is statically unobservable. Furthermore, the implicit Euler appears to have a more damped response to slightly wrong initial conditions, whereas the trapezoidal rule achieves slightly better tracking during transients.

The maximal number of iterations to reach the prespecified threshold of  $\epsilon = 10^{-4}$  and the average and worst-case computing times for the iterated schemes are shown in Table I. Both the average and the worst-case computing times are significantly lower than the PMU sampling rate, which renders

the method suitable for real-world applications.

In what follows, we only consider the trapezoidal discretization scheme, as its tracking performance during transients is deemed superior to the forward and backward Euler. Fig. 4 presents the true and the estimated voltage magnitudes of all nodes in the shaded area. The estimated states closely track the true values, both during steady state and transients. The average mean-square error of the estimation of all nodes after the initialization phase ( $t \geq 7.5$  s) is  $8.25 \cdot 10^{-7}$ . This value is smaller than the variance of the PMU measurement noise, despite the fact that the network is statically unobservable.

### C. Case Study 2: Load Disturbance

To compare the proposed method with the existing methods in the literature, we simulate a step change of the load consumption at node 21, mimicking a sudden disconnection of a large consumer. For comparison, we employ a decoupled approach from the literature, wherein in the first stage, a static estimator calculates the voltages in the grid. As the network is not observable with the given PMU configuration, additional power pseudo-measurements are used for all the loads and for the interface node 16. These values can be obtained, for example, from historical data or from slow scan rate conventional measurements and correspond to the actual operating point before the disturbance. With more uncertainty regarding those values compared to the PMU measurements, the static state estimator is implemented with a robust least absolute value procedure (LAV). In the second stage, to estimate the differential states of the generators, the EKF with two additional states to address the noise in the input vector and the  $H_\infty$  EKF (HEKF) [49] are implemented. The terminal voltages are used as inputs and the terminal currents as measurements. The results in Fig. 5 highlight that all three methods accurately track the system states before the disturbance at  $t = 8$  s. However, after the disturbance, the two-stage approaches exhibit an error due to the unexpected load change.

## V. CONCLUSIONS AND FUTURE WORK

A novel centralized DSE has been proposed to address potential incompleteness of the power system model. The proposed approach is performed as an iterative procedure that generalizes the IEKF without any prior knowledge or assumptions about some of the injectors. Nevertheless, the estimation of all system states was demonstrated to be very accurate when the estimability condition was fulfilled. It was shown that estimability is satisfied topologically if all unknown injectors can be connected to a PMU device by disjoint paths. The numerical results showcase the importance of the employed discretization scheme for DSE with an incomplete nonlinear DAE model, and the moderate computing times of the proposed scheme signify real-time feasibility. The proposed method outperforms the robust two-stage decoupled methods from the literature during sudden disturbances. While the usefulness of DSE is still being debated (see [50]), we argue that it will be crucial to provide reliable estimates during abnormal operating conditions to enable time-critical



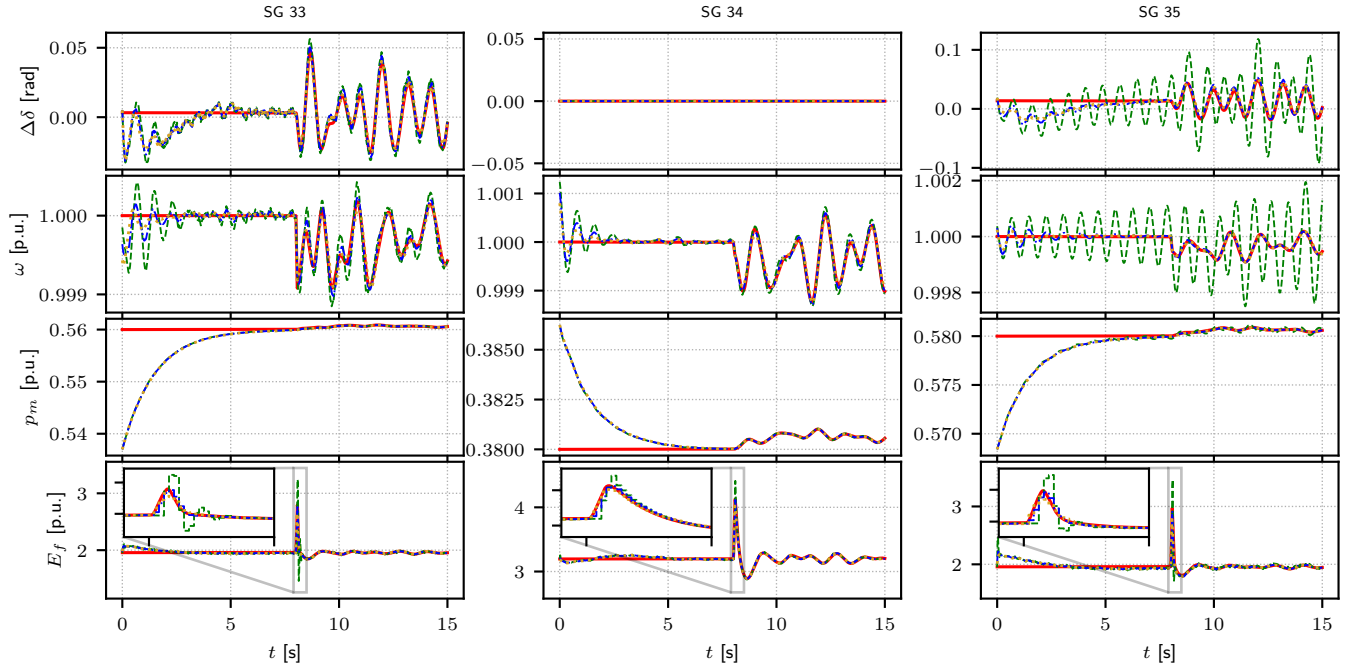


Fig. 3. Results of estimation of dynamic states of SGs during initialization and during and after the short-circuit in the network. The true state is denoted by  $\text{---}$ ; the proposed IEKF with the forward Euler is denoted by  $\text{- - -}$ , with the trapezoidal rule by  $\text{- - -}$ , and with the backward Euler by  $\text{. . .}$ . From top to bottom: rotor angle, rotor speed, turbine power, exciter voltage; from left to right: SG 33, SG 34, and SG 35.

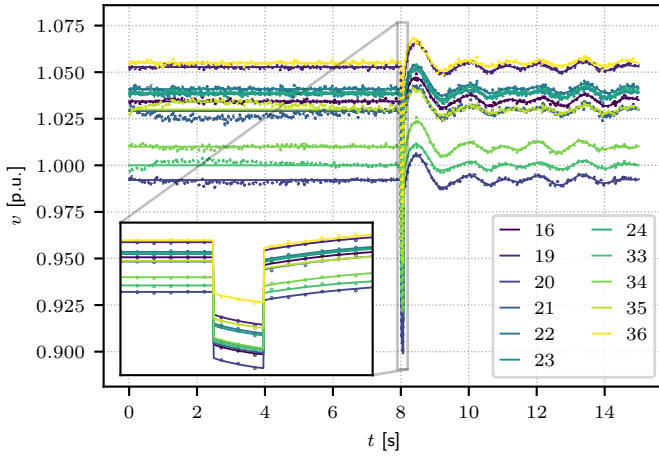


Fig. 4. Results of estimated and true voltage magnitudes during the initialization and during and after the short circuit. Full lines denote the true voltages; markers denote the estimated ones using the trapezoidal discretization.

control and protection, particularly because the power grids are expected to be operated closer to their security margins in the future [51].

There are several immediate extensions of this work. Including decentralized power electronics-interfaced generation and evaluating the performance under altered system dynamics is an obvious direction for further research. In addition, it would be interesting to theoretically analyze the convergence of the recursive scheme and design an optimization algorithm for the optimal placement of PMUs. Finally, even though the method can disregard the injectors with unknown models or those whose behavior does not comply with the theoretical

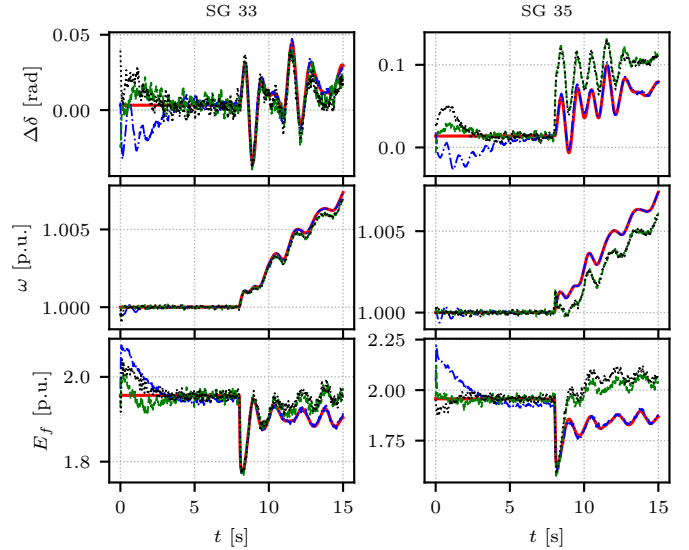


Fig. 5. Results of the comparison of the proposed method  $\text{- - -}$  with the two-stage approach from the literature: LAV+EKF  $\text{- - -}$  and LAV+HEKF  $\text{- - -}$ . The true state is represented by  $\text{---}$ .

expectations, bad data can still appear, either in the form of innovation or observation outliers. Therefore, future work will also address the detection and identification of bad data.

## REFERENCES

- [1] A. Abur and A. Expósito, *Power System State Estimation: Theory and Implementation*. Power Engineering (Willis), CRC Press, 2004.
- [2] E. Farantatos, "Questions and Answers- Let's Talk About Synchrophasors, PMUs & Applications." <https://www.naspi.org/node/822>. Accessed: 2022-11-23.

- [3] E. Scholtz, *Observer-based Monitors and Distributed Wave Controllers for Electromechanical Disturbances in Power Systems*. Massachusetts Institute of Technology, Department of Electrical Engineering and Computer Science, 2004.
- [4] A. K. Singh and B. C. Pal, *Dynamic Estimation and Control of Power Systems*. Elsevier, 2019.
- [5] E. Ghahremani and I. Kamwa, "Dynamic state estimation in power system by applying the extended Kalman filter with unknown inputs to phasor measurements," *IEEE Transactions on Power Systems*, vol. 26, no. 4, pp. 2556–2566, 2011.
- [6] J. Qi, K. Sun, J. Wang, and H. Liu, "Dynamic state estimation for multi-machine power system by unscented Kalman filter with enhanced numerical stability," *IEEE Transactions on Smart Grid*, vol. 9, no. 2, pp. 1184–1196, 2018.
- [7] Y. Cui and R. Kavasseri, "A particle filter for dynamic state estimation in multi-machine systems with detailed models," in *2016 IEEE Power and Energy Society General Meeting (PESGM)*, pp. 1–1, 2016.
- [8] S. Wang, W. Gao, and A. P. S. Meliopoulos, "An alternative method for power system dynamic state estimation based on unscented transform," *IEEE Transactions on Power Systems*, vol. 27, no. 2, pp. 942–950, 2012.
- [9] J. Qi, K. Sun, J. Wang, and H. Liu, "Dynamic state estimation for multi-machine power system by unscented Kalman filter with enhanced numerical stability," *IEEE Transactions on Smart Grid*, vol. 9, no. 2, pp. 1184–1196, 2018.
- [10] J. Qi, K. Sun, and W. Kang, "Optimal PMU placement for power system dynamic state estimation by using empirical observability gramian," *IEEE Transactions on Power Systems*, vol. 30, no. 4, pp. 2041–2054, 2015.
- [11] A. Rouhani and A. Abur, "Linear phasor estimator assisted dynamic state estimation," *IEEE Transactions on Smart Grid*, vol. 9, no. 1, pp. 211–219, 2018.
- [12] M. Nadeem, S. A. Nugroho, and A. F. Taha, "Dynamic state estimation of nonlinear differential algebraic equation models of power networks," *IEEE Transactions on Power Systems*, pp. 1–14, 2022.
- [13] M. Nadeem and A. F. Taha, "Robust dynamic state estimation of multi-machine power networks with solar farms and dynamics loads," 2022.
- [14] C. R. Fuerte-Esquivel, O. Romay, R. Martinez-Parrales, E. Acha, and E. A. Zamora-Cardenas, "A new dynamic state estimation approach including hard limits on control devices," *IEEE Transactions on Power Systems*, pp. 1–1, 2022.
- [15] M. Katanic, J. Lygeros, and G. Hug, "Moving-horizon state estimation for power networks and synchronous generators," in *2022 North American Power Symposium (NAPS)*, pp. 1–6, 2022.
- [16] J. Zhao, A. Gómez-Expósito, M. Netto, L. Mili, A. Abur, V. Terzija, I. Kamwa, B. Pal, A. K. Singh, J. Qi, Z. Huang, and A. P. S. Meliopoulos, "Power system dynamic state estimation: Motivations, definitions, methodologies, and future work," *IEEE Transactions on Power Systems*, vol. 34, no. 4, pp. 3188–3198, 2019.
- [17] S. Abhinav and B. Pal, *Dynamic Estimation and Control of Power Systems*. Elsevier Science, 2018.
- [18] J. Zhao, M. Netto, and L. Mili, "A robust iterated extended Kalman filter for power system dynamic state estimation," *IEEE Transactions on Power Systems*, vol. 32, no. 4, pp. 3205–3216, 2017.
- [19] J. Zhao, "Dynamic state estimation with model uncertainties using  $H_\infty$  extended Kalman filter," *IEEE Transactions on Power Systems*, vol. 33, pp. 1099–1100, 2018.
- [20] J. Zhao and L. Mili, "Robust unscented Kalman filter for power system dynamic state estimation with unknown noise statistics," *IEEE Transactions on Smart Grid*, vol. 10, no. 2, pp. 1215–1224, 2019.
- [21] Y. Li, J. Li, J. Qi, and L. Chen, "Robust cubature Kalman filter for dynamic state estimation of synchronous machines under unknown measurement noise statistics," *IEEE Access*, vol. 7, pp. 29139–29148, 2019.
- [22] W. Wang, C. K. Tse, and S. Wang, "Dynamic state estimation of power systems by  $p$ -norm nonlinear Kalman filter," *IEEE Transactions on Circuits and Systems I: Regular Papers*, vol. 67, no. 5, pp. 1715–1728, 2020.
- [23] S. Wang, R. Huang, Z. Huang, and R. Fan, "A robust dynamic state estimation approach against model errors caused by load changes," *IEEE Transactions on Power Systems*, vol. 35, no. 6, pp. 4518–4527, 2020.
- [24] F. Feng, Y. Zhou, and P. Zhang, "Neuro-dynamic state estimation for networked microgrids," 2022.
- [25] S. Golejani and M. T. Ameli, "A multi-agent based approach to power system dynamic state estimation by considering algebraic and dynamic state variables," *Electric Power Systems Research*, vol. 163, pp. 470–481, 2018.
- [26] J. Ishihara, J. Campos, and M. Terra, "Optimal recursive estimation for discrete-time descriptor systems," in *Proceedings of the 2004 American Control Conference*, vol. 1, pp. 188–193 vol.1, 2004.
- [27] R. Nikoukhah, A. Willsky, and B. Levy, "Kalman filtering and Riccati equations for descriptor systems," *IEEE Transactions on Automatic Control*, vol. 37, no. 9, pp. 1325–1342, 1992.
- [28] V. A. Aryasomyajula, N. Gatsis, and A. F. Taha, "Power system dynamic state estimation based on discretized nonlinear differential algebraic equation models," in *2022 North American Power Symposium (NAPS)*, pp. 1–6, 2022.
- [29] M. Mahzouni Sani, *Dynamic State Estimation in Power Systems Using Implicit Discretization Methods*. PhD thesis, University of Texas San Antonio, 2021.
- [30] B. Stott, "Power system dynamic response calculations," *Proceedings of the IEEE*, vol. 67, no. 2, pp. 219–241, 1979.
- [31] A. Jovicic and G. Hug, "Linear state and parameter estimation for power transmission networks," in *2020 International Conference on Probabilistic Methods Applied to Power Systems (PMAPS)*, pp. 1–6, 2020.
- [32] M. Z. Boulaïd Boulkroune, Mohamed Darouach, "Moving horizon state estimation for linear discrete-time singular systems," *IET Control Theory and Applications, Institution of Engineering and Technology*, vol. 4, no. 3, pp. 339–350, 2010.
- [33] D. Simon, *Optimal State Estimation: Kalman, H Infinity, and Nonlinear Approaches*. Wiley, 2006.
- [34] M. Göhl and A. Abur, "LAV based robust state estimation for systems measured by PMUs," *IEEE Transactions on Smart Grid*, vol. 5, no. 4, pp. 1808–1814, 2014.
- [35] B. Bell and F. Cathey, "The iterated kalman filter update as a gauss-newton method," *IEEE Transactions on Automatic Control*, vol. 38, no. 2, pp. 294–297, 1993.
- [36] L. Dai, *Singular Control Systems*. Lecture Notes in Control and Information Sciences, Springer Berlin Heidelberg, 2014.
- [37] T. B. Gross, S. Trenn, and A. Wirsen, "Topological solvability and index characterizations for a common DAE power system model," in *2014 IEEE Conference on Control Applications (CCA)*, pp. 9–14, 2014.
- [38] G. R. Krumpholz, K. A. Clements, and P. W. Davis, "Power system observability: A practical algorithm using network topology," *IEEE Transactions on Power Apparatus and Systems*, vol. PAS-99, no. 4, pp. 1534–1542, 1980.
- [39] E. Scholtz and B. C. Lesieutre, "Graphical observer design suitable for large-scale DAE power systems," in *2008 47th IEEE Conference on Decision and Control*, pp. 2955–2960, 2008.
- [40] S. Hosoe, "Determination of generic dimensions of controllable subspaces and its application," *IEEE Transactions on Automatic Control*, vol. 25, no. 6, pp. 1192–1196, 1980.
- [41] I. Hiskens, "IEEE PES Task Force on Benchmark Systems for Stability Controls," tech. rep., IEEE Power & Energy Society, 2013.
- [42] J. Machowski, Z. Lubosny, J. W. Bialek, and J. R. Bumby, *Power System Dynamics: Stability and Control*. Wiley, 2020.
- [43] "Dynamic models for turbine-governors in power system studies," tech. rep., IEEE Power & Energy Society, 2013.
- [44] P. Kundur, N. Balu, and M. Lauby, *Power System Stability and Control*. EPRI power system engineering series, McGraw-Hill Education, 1994.
- [45] P. Sauer and M. Pai, *Power System Dynamics and Stability*. Prentice Hall, 1998.
- [46] F. Milano, *Power System Modelling and Scripting*. Power Systems, Springer Berlin Heidelberg, 2010.
- [47] "IEEE standard for synchrophasor data transfer for power systems," *IEEE Std C37.118.2-2011 (Revision of IEEE Std C37.118-2005)*, pp. 1–53, 2011.
- [48] J. A. E. Andersson, J. Gillis, G. Horn, J. B. Rawlings, and M. Diehl, "CasADi – A software framework for nonlinear optimization and optimal control," *Mathematical Programming Computation*, vol. 11, no. 1, pp. 1–36, 2019.
- [49] J. Zhao, "Dynamic state estimation with model uncertainties using  $h_\infty$  extended kalman filter," *IEEE Transactions on Power Systems*, vol. 33, no. 1, pp. 1099–1100, 2018.
- [50] J. Zhao, M. Netto, Z. Huang, S. S. Yu, A. Gómez-Expósito, S. Wang, I. Kamwa, S. Akhlaghi, L. Mili, V. Terzija, A. P. S. Meliopoulos, B. Pal, A. K. Singh, A. Abur, T. Bi, and A. Rouhani, "Roles of dynamic state estimation in power system modeling, monitoring and operation," *IEEE Transactions on Power Systems*, vol. 36, no. 3, pp. 2462–2472, 2021.
- [51] F. Milano, F. Dörfler, G. Hug, D. J. Hill, and G. Verbič, "Foundations and challenges of low-inertia systems," in *Power Systems Computation Conference (PSCC)*, pp. 1–25, 2018.